

Assessing local acid mine drainage impacts on natural regeneration-revegetation of São Domingos mine (Portugal) using a mineralogical, biochemical and textural approach

Renata A. Ferreira^{a,*}, Manuel F. Pereira^{b,1}, João P. Magalhães^c, António M. Maurício^b, Isabel Caçador^c, Susete Martins-Dias^d

^a CERENA, Instituto Superior Técnico, Universidade de Lisboa, Av. Rovisco Pais, 1049-001 Lisboa, Portugal

^b CERENA, DECivil, Instituto Superior Técnico, Universidade de Lisboa, Av. Rovisco Pais, 1049-001 Lisboa, Portugal

^c MARE, Faculdade de Ciências, Universidade de Lisboa, 1749-016 Lisboa, Portugal

^d CERENA, DBE, Instituto Superior Técnico, Universidade de Lisboa, Av. Rovisco Pais, 1049-001 Lisboa, Portugal

*Corresponding author.

E-mail addresses: renata.ferreira@tecnico.ulisboa.pt (R.A. Ferreira), mfcp@tecnico.ulisboa.pt (M.F. Pereira), joao.magalhaes@tecnico.ulisboa.pt (J.P. Magalhães), pcd2045@tecnico.ulisboa.pt (A.M. Maurício), micacador@fc.ul.pt (I. Caçador), susetedias@tecnico.ulisboa.pt (S. Martins-Dias).

¹Authors contribute equally to this work.

HIGHLIGHTS

- Integrated approach highlighted the AMD repercussions in non-vegetated areas.
- Old discharging areas of wastewaters revealed low toxicity and ecosystem regeneration.
- Flood deposit has a very acidic and aluminous top layer critical to plant growth.
- * Jarosites s.l. seems to be the main hazardous metal(loid)s mineral carrier.
- São Domingos AMD proximal and distal places demand distinct revegetation solutions.

GRAPHICAL ABSTRACT



Editor: Filip M.G. Tack

Keywords:

Abandoned mines
Hypersaline deposits
Jarosite
Phytoremediation
Phytotoxicity

ABSTRACT

São Domingos sulfide mine was shut down more than 50 years ago leaving behind eroded and depositional surfaces due to acid mine drainage (AMD). The aim of this study was to assess six selected sites subjected to AMD, considered phytotoxic regions characterized by vegetation scarcity. Two main criteria, nature and composition of soluble fractions and total chemistry of surficial products related to jarosites presence, enabled to set up an overall dichotomy between superficial proximal/discharge and distal/sedimentation areas. Wet and dry sieving results comparison revealed that samples have a predominant sandy texture and lithic (phyllite, quartzite and volcanic country rocks) composition. Quartz, and subordinate feldspar enrichment is also detected in the coarse silt fraction. The results also suggest that the materials under study, when subjected to the local torrential hydrologic regime, have a high mechanical vulnerability, facilitating erosion and mud transport, both critical for vegetation support, and triggering contamination transfer and dispersion. The vicinity and ground-level surfaces of discharging areas are enriched in the jarosite group minerals whereas the sedimentation ones present hypersaline aluminous tendency. The formation of jarosite is considered as an efficient positive environmental contribution to metals and metalloids sequestration/immobilization. The remediation/vegetation solutions to be adopted in each location must have into consideration these differentiating aspects.

1. Introduction

Abandoned mines are a worldwide environmental concern due to the large amount of rejects left in the open air often leading to the production of acid mine drainages (AMD), responsible for soils contamination, surface and groundwater bodies with a wide range of pollutants, including trace metal(loid)s, which revealed to be harmful to ecosystems in the mine's surroundings (Bini, 2011). Located in the SE part of Portugal, in the northern part of the Iberian Pyrite Belt (IPB), distant about 5 km from the Spanish border, the inactive sulfide mine of São Domingos constitutes no exception. Here, a large area was affected by a large variety of mining and metallurgical activities that lasted for more than a hundred years (1857-1966) (Álvarez-Valero et al., 2008; Pérez-López et al., 2008).

The ore leaching fields, the crushing mills of Moitinha and the sulfur production plants of Achada do Gamo are located downstream from the mining strip, and along the valley of the São Domingos stream. Between this industrial area and the Chumbeiro dam, located about 5 km downstream, there are large non-vegetated areas affected by AMD, due to the sulfide processing methods and the control of acidic waters along with a vast mining channel/dam systems (Matos et al., 2006; Matos et al., 2012). Residual water discharges from slope channels promoted water decontamination, by contact with the percolated rocks, and minimized their flow (essentially through evaporation).

The leaching of mining wastes by rainwater generates acidic waters rich in soluble metals that impact the water quality of Ribeira de São Domingos (a tributary of the Chança River) while being transported downstream to the main water receiving body, the Guadiana River (Álvarez-Valero et al., 2008). This kind of contamination can be recognized in many IPB sites, namely in the Portuguese part (e.g., Lousal, Caveira and Aljustrel). The presence of secondary minerals in mining affected areas is indicative that these materials are still reactive (Álvarez-Valero et al., 2008). Secondary paragenesis, mainly sulfates with different compositions,

crystalline degree and solubility, as well neof ormation silicates, oxides and hydroxides control the bioavailability of chemical elements, and their inherent toxicity risks threatening the surrounding environment (Álvarez-Valero et al., 2008; Sánchez España et al., 2005; Matos et al., 2006). This is particularly important in AMD related to solid wastes containing pyrite or to acidic water percolation in other mining tailings (Álvarez-Valero et al., 2008). Soils and other surficial deposits are very heterogeneous. They were mainly developed on weathered rocks, more or less mixed with waste materials of various compositions, and riverbank sediments leading to abroad soil pH range (1.8-7.8), as reported by Abreu et al. (2012). Moreover, geochemical research showed anomalous content of Pb, As, S, Cu, Cd, and Hg in soils and of Zn, Pb, Sb, Cu, Ag, Hg, and Cd in tailing materials (Abreu et al., 2012). According to our observations, and many other studies performed in São Domingos mining site, the pollution dissemination and the contamination dynamics by the residues have been continuous and triggered by the cyclical dissolution process of the trace metal(loid)s fraction during the rainy seasons (Rosado et al., 2008). In warmer seasons, one part of the AMD- pollutants is kept by precipitation of evaporitic salts, being re-dissolved in rainy periods (Álvarez-Valero et al., 2008).

Historical data indicates that acid residual mining waters, coming from different mining and metallurgical operations, were diverted to an artificial channel-dam system in an attempt to control the volume of contaminated water discharges into the São Domingos stream and the Chança River (Matos et al., 2006; Álvarez-Valero et al., 2008). Channel discharges of residual acid waters were done, during an unknown period, to promote water evaporation and pH increase. Due to the end of the mining activity in 1966, this process came to a halt and, since then, the system has been evolving naturally. Given that natural processes overlap in a very intense and complex way with anthropogenic processes, this constitutes an environmental problem although mitigated by the fact that the main source of contamination stopped with the closure of the mine (Álvarez-Valero et al., 2008; Pérez-López et al., 2008).

Currently, the São Domingos mine region is subject of great scientific, landscape architectural, touristic, geoparking and environmental challenge/relevance (in 2013 the mine and the urban area of São Domingos was classified by the Portuguese authorities as a “Set of Public Interest” (visitmertola, 2015)). The development strategy applied by Empresa de Desenvolvimento Mineiro, S.A. (EDM; a company responsible for environmental passive recovery in degraded mining areas in Portugal) seeks for solutions to the environmental problems and for the mining heritage preservation and valorization of the site (GPGMS, 2020). With the final objective of reducing the volume of acidic waters up to 84%, EDM is promoting the construction of channels on the Western banks and on the Eastern valley slopes and banks to collect/deviate the non-contaminated surface water (EDM, 2019). The environmental remediation of the São Domingos mining area is an on-going process (with the help of several multidisciplinary research teams).

The São Domingos mining area suffers from a more intense chemical and physical weathering compared to non-contaminated areas due to the artificially and more acidified environment exposure to the local Mediterranean climate, characterized by hot, dry summers and fairly rainy winters (Rosado et al., 2008). Indeed, climatic conditions might accelerate the weathering rate of unstable minerals, leading to an increase of chemical toxicity in plant rhizosphere and thus discontinuing a natural revegetation process on mine tailing areas (Huang et al., 2012). The acids, metal(loid)s and other hazardous elements released by weathering can be stored in part as salt minerals and/or dissolved and transported by runoff or soil percolation. Thus, efflorescent and/or inflorescent salt composition can indicate at least some of the overall chemical processes involved in rock-soil-water interactions (Murray et al., 2014). Moreover, in highly acidic and oxidizing environments such as these, the retention and mobilization of toxic metals can be affected by the local overburden deposits composition (Huang et al., 2012; Dold, 2014).

Several plant species belonging to the genera *Cistus* and *Erica* colonize São Domingos mine areas rich in hazardous chemical elements showing no signs of toxicity or accumulation of metal(oid)s (such as As, Sb, and Pb) which indicates that they are phytotolerant species.

Moreover, the mitigation strategies of the physical and chemical soil features that hinder the hydro-geochemical conditions for plant root establishment and development, and the proliferation of soil biota in the long term should be taken into account (Huang et al., 2012). To that purpose Abreu et al. (2012) suggested the use of autochthonous herbaceous species, e.g., *Cistus* sp. or *Erica* sp., to promote the xerosere evolution and the natural regeneration processes of weathering and pedogenesis.

In the field, the most notable aspect of AMD is the rock substrate strong degradation that produces coloration and covers the area with powdered loose materials. With the aim of contributing to set-up a valid revegetation and/or phytoremediation strategy of those areas, our assessment was done in different locations where no established vegetation can currently be found. However, it can be found in or near these contaminated areas, AMD isolated and preserved native flora regions (see supplementary material Fig. S1), that can be used for reference studies.

Metal(loid)s toxicity to the ecosystem is difficult to establish due to the intricate network that contributes to metals speciation, mobility potential and effective bioavailability. In general, it is well known that exposure to a high heavy metal concentration is potentially toxic to all living beings, including microorganisms and plants, interfering with their metabolism (Bååth, 1989). The toxicological effect on soil microorganisms diminishes the soil quality and soil biochemical properties, due to microbial growth and enzyme activity inhibition. Soil quality has been successfully assessed from the activity of extracellular enzymes excreted by bacteria, fungi, and plants selected as bioindicators with prompt sensitivity to environmental stress and soil conditions (Turner et al., 2002). However, each enzyme activity is related to specific reactions and is substrate specific, so, to ascertain e.g. the biochemical fertility of a soil, it is necessary to measure the activity of a group of enzymes (Alkorta et al., 2003). Enzymes such as (β -glucosidase (BGL), dehydrogenase (DH), acid phosphomonoesterase (APM) and arylsulphatase (AS) are often described in the literature as good soil quality indicators (von Mersi and Schinner, 1991; Paz-Ferreiro et al., 2011).

Given this general framework, the focus of this study is placed on the referred non-vegetated areas affected by AMD. To promote better management tools to enable the rehabilitation of those areas it is imperative to assess, together with field observations, their characteristics (texture and mineralogical composition), enabling a better study of the mechanisms behind their toxicity to the local flora and their vulnerability. This is in order to clarify whether the natural biogeochemical-physical regeneration/recuperation processes (influencing the contaminated area geomorphology dynamics) are being disturbed.

Taking into account that a better characterization enables the vulnerability and risk mapping of contaminated areas of different typologies possible, results from this research may also be used in designing future selection and application of better phytoremediation strategies, not only at the São Domingos area (which is the main goal of our project PhytoCharMe), but also in other equally complex systems of the same type.

2. Materials and methods

2.1. Site description and sampling

São Domingos abandoned mine is one of the volcanogenic massive sulfide deposits situated within the Iberian Pyrite Belt, which extends from Spain along the south region of Portugal, in Baixo Alentejo Province. The climate of the area is of a Mediterranean type, that alternates between long warm-dry periods and short but intense rainy periods. Nonetheless, two periods can be noticed: a wet period from November to April and a dry period from May to September. In the region, the averages of the minimum air temperatures varies between 5 and 16 °C, the averages of the maximum air temperatures varies between 14 and 33 °C and the average of the annual precipitation varies between 500 and 600 mm (IPMA, 2020).

In the area adjacent to the mine, there are several plant species well adapted to the peculiar mining and metallurgical habitat. Among these species, *Cistus ladanifer*, *Cistus monspeliensis*, *Cistus salvifolius*, *Lavandula stoechas*, *Agrostis castellana* and *Erica australis* were observed. In wet areas around the banks of lagoons, which resulted from mining activity, occurs *Erica andevalensis*. This is an Iberian endemism and a critically endangered species included in UCN Red List (Buira et al., 2019).

Six surface layer samples (S1 to S6; see Fig. 1 and in supplementary material Fig. S1) from areas that presented scarce or no vegetation were collected across the São Domingos mine site at the following locations: S1: 37°38'33.28"N, 7°30'38.24"W, S2: 37°38'31.78"N, 7°30'41.01"W, S3: 37°38'31.15"N, 7°30'40.92"W and S4: 37°38'32.82"N, 7°30'41.72" W, all near the Achada do Gamo sulfur factories, S5: 37°38'7.89"N, 7°30'43.86"W nearby Chumbeiro dam and S6: 37°39'1.73"N, 7°30'45.59"W near the Moitinha ore mills. The selected sampling sites are in accordance with the main goal of defining a revegetation strategy for both western and eastern slopes of the São Domingos stream valley.

Samples of ca. 2 kg, within a 225 cm² boundary and up to 15 cm depth, were collected in each location and carried to the laboratory in sealed plastic containers. AMD decomposed outcrop rock samples were also collected in S1 site and were defined as S1RA and S1RB. Grayish and yellowish saline crusts, as well as alower ocher level layer, were taken separately in S2 location.

According to a previous mining area zonation (Álvarez-Valero et al., 2008) the gathered samples were included in “unvegetated areas affected by extreme acid mine drainage”. The S2 and S3 samples can be considered as “leached materials in seasonal flooded areas”. Quental et al. (2003), using hyperspectral images analysis,

included: S2 and S3 location in a “mixture of materials rich in sulfur”; S1 in a “reddish or yellowish ferricrete” category; S4 in a location close to the “mixture leached rock fragments” unit; S5 in the “outcrop of leached rock with white tone” unit; and S6 location in a mixture of leached rocks, ferricretes, and contaminated soils and sediments.

Considering fieldwork observations in the sites under studying, the proposed ferricrete categories are not adequate. Thus, a more detailed categorization for the sampled sites is proposed: (a) S1 and S5 can be considered as an acid drainage leached rock outcrop slope domain, with limited and sparse industrial solid wastes at surface. Rock formations show singular weathering and erosional features (combined effects of coloration, delamination, exfoliation and rounding). We suggest that part of these areas should be preserved as scientific or natural heritage. (b) S2 and S3 sample sites belong to an old flooded acid drainage deposition related to an abandoned local dam, located in the eastern slope of São Domingos stream. This dam was used to control wastewater discharges to the São Domingos stream but at this moment it is filled with sediments. A saline crust showing grayish and yellowish tones is visible (Fig. 1). (c) S4 is separated from S2 and S3 samples by an earth dam containment barrier (complex industrial wastes with apparently low pyrite content). Its composition can be dependent on the AMD sediment accumulation from slope erosion and local tailings leaching. (d) S6 location is alike S1 and S5 sites but presenting a lower slope. AMD leached superficial deposition is then thicker. In the central region of the studied area (see supplementary material Fig. S1) where four samples were taken (S1 to S4), it was possible to develop a more integrated study from the geochemical and environmental points of view. Field observations and Google Earth satellite images show, that the water line after the dam, and in the continuity of the sedimentary flood deposit, has a limited presence of salts and colorations. These aspects indicate that the system is no longer strongly affected by AMD and that the sparsity of the vegetation along this water line is correlated with the water regime.

2.1.1. Sample preparation

After arrival at the laboratory, all samples were spread on trays and air-dried at room temperature for one week. Afterwards, each sample was pulled together, weighted and manually sieved. Gravel particles >3.15 mm were not selected to further detailed granulometric analysis.

The powdery texture and/or salty nature of samples only allow minor macroscopic observations. So, bearing in mind the large contribution of the lithic fragments observed on samples, and the main objective of this study, the wet manual sieving was considered pertinent. Indeed, manual gentle wet sieving enables: (1) the macroscopically visualization and identification of samples main coarse constituents with minor mechanical interference (induced aggregate/water separation, particle dispersion and classification) and its granulometric analysis; (2) the microscopically identification of fine constituents and its separate granulometric analysis; (3) the extraction and analysis of the soluble salts and/or sorbed trace elements (e.g. of precipitated salts and/or trace metal(oid)s); (4) the identification of the contamination sources



Fig. 1. São Domingos collected samples map location. A partial mining area general view is presented on the top and, the taken pictures of the sampling sites are shown on the bottom. Drainage channels, visible in the middle of the slopes (on the top image), are the source of historical acid mine drainage discharges in the studied areas. S1-37°38'33.28"N, 7°30'38.24"W; S2-37°38'31.78"N, 7°30'41.01"W; S3-37°38'31.15"N, 7°30'40.92"W; S4-37°38'32.82"N, 7°30'41.72"W; S5-37°38'7.89"N, 7°30'43.86"W; S6-37°39'1.73"N, 7°30'45.58"W. White circles have 300 m diameter.

(natural or anthropogenic) and processing of separated phase or anomaly analysis; (5) mimicking a natural process of sample wet transport in order to predict at least part of the erosion processes and plant ground stability. Together the gathered information is considered very relevant to improve knowledge about future intervention areas and proposals for revegetation solutions.

Consequently, the <3.15 mm air-dried samples were divided into two subsamples and stored in hermetic plastic bags for further analysis (one for dry sieving and the other for manual washing and sieving).

2.2. Sample sieving

2.2.1. Dry sieving

Dry sieving (DS) was accomplished with a mesh set no. 10, 20 and 200 (2.0, 0.85 and 0.075 mm, respectively), and then weighted following (ASTM, 2001). All sieved fractions were hermetically stored at room temperature, apart from a portion of the <2 mm sample fraction that was stored at 4 °C (to be used in the sample quality assessment; Paz-Ferreiro et al., 2009).

2.2.2. Manual washing and sieving

Manual gentle washing sieving (WS) was performed with a mesh set no. 8, 10, 15, 20, 40, 70, 120, 200, 230 and 500 (2.36, 2.0, 1.0, 0.85, 0.425, 0.212, 0.125, 0.075, 0.063 and 0.025 mm, respectively) following (ASTM, 2014; WS, 2020). This process took around one hour for each sample. The fractions were oven-dried at 40 °C during 48 h, cooled down, weighted, and hermetically stored at room temperature. The water used for the sieving process was collected and after complete decantation, the soluble fraction was oven-dried at 30 °C until total evaporation, and corresponding salt formation. The salt identification provides an indirect way of knowing the chemistry of the most mobile components of the system but is limited to the existing crystalline species and their stability. All these fractions were observed and characterized under stereomicroscope and representative captures were taken.

2.3. Physical-chemical analysis

The sample pH, electrical conductivity (EC), moisture content (M) and loss on ignition (LOI) were assessed in the <2 mm sample fraction obtained after dry sieving. All assays were performed in triplicate. The pH was measured in a suspension of 10 g of the sample fraction in 25 ml of distilled water, according to the method described by Carter and Gregorich (2007). The same procedure was applied to the rock samples collected at S1 site. EC was measured in the same suspensions prepared for the pH determination, after a settling period of 24 h. The sample M was determined from the loss of weight after drying at 105 °C (on average, after 4 h) and LOI was determined by weight loss on ignition at 450 °C, during 8 h (Pereira et al., 2008; LOIP, 2020).

São Domingos samples elemental content was determined in the <0.075 mm fraction obtained after dry sieving. The <0.075 mm fractions were hermetically stored in plastic tubes and sent for analysis to Activation Laboratories Ltd. (Ancaster, Ontario, Canada; method code - EUT1 (ICP-MS)).

2.4. Sample quality assessment

The sample quality assessment was achieved through the determination of the enzymatic activities of BGL, APM, AS and DH, using 0.5 g dry weight of the 2 mm dried sieved fractions (stored at 4 °C).

The BGL activity was quantified based on the method of Eivazi and Tabatabai (1988), but using 25 mM *p*-nitrophenyl- β -D-glucopyranoside as substrate and modified universal buffer (MUB; (Stotzky et al., 1993)) at pH 5 as described by Paz-Ferreiro et al. (2009). The activity of APM was determined following the method of Tabatabai and Bremner (1969). The AS activity was determined as described by Tabatabai and Bremner (1970). The specific enzymatic activities of BGL, APM and AS were quantified by reference to a calibration curve corresponding to *p*-nitrophenol (pNP) standards absorbance at 400 nm and expressed in $\mu\text{g pNP g}^{-1}\text{ soil dw h}^{-1}$, at 37°C (Tabatabai and Bremner, 1969).

The activity of DH was determined following Alef and Nannipieri (1995) with minor changes according with Camiña et al. (1998). Briefly, the concentration of iodinitrotetrazolium (INT) used was 4.94 mM. After the extractant addition, the reaction mixture was incubated in the dark for 10 min, at 40 °C. The specific activity of DH was quantified by reference to a calibration curve corresponding to iodinitrotetrazolium formazan (INTF) standards absorbance at 490 nm, expressed in $\mu\text{g INTF g}^{-1}\text{ soil dw h}^{-1}$, at 40 °C (Alef and Nannipieri, 1995).

The spectrophotometric enzymatic assays were performed using a microplate reader equipped with temperature controller (Cary 50 Bio, VARIAN®). In all the activity assays, prior the reaction spectrophotometric reading, the filtration step of the reaction mixture was replaced by a centrifuging step, at 1500g during 10 min at room temperature, according to Turner et al. (2002). The solutions and buffers were prepared with high chemical grade reagents and ultra-pure water (Milli-Q, Millipore®). All values reported are averages of three determinations.

2.5. Mineralogical analysis

After the visual inspection, was considered for mineralogical analysis the following fractions of each sample: (1) DS<0.075 mm; (2) WS>1mm, (3) WS <0.025 mm. The leached and further precipitated soluble salts resultant from the WS separation process were also analyzed. Rock compositions and soluble salts were also characterized, as well as saline crusts from sample S2. The identification and semi quantification of the sample's mineral phases and its leached salts were carried out by X-Ray diffraction (XRD; Panalytical X'PERT PRO diffractometer). The analysis was accomplished with CuK α source (35 mA, 40 kV), between 5° and 70° 2 θ , with 0.0330° 2 θ step size and 75 s scan step time. For low crystallinity products analysis, a higher scan time was used (150 to 200 s) as indicated by Sánchez España et al. (2005). The identification phase was performed with Highscore Plus software using the PDF2® data base.

3. Results and discussion

3.1. Sample characterization

3.1.1. Textural analysis

The <3.15 mm particle size distribution results from the DS and from the WS of the samples (S1 to S6) are presented in Fig. 2. Results indicate that significant textural changes can occur, when comparing DS and WS products, even in sand-gravel textural dominant samples. Gravel and coarse sand fractions of all samples had suffered a significant reduction upon WS. The exception was sample S3. The percentage of fines (fraction <0.075 mm) is much higher after WS than DS for most samples, due to its powdery and cloddy structure (in S1, S4, S5 and S6 <0.075 mm WS fractions exceed 30%).

By comparing the particle size distribution of the two applied sieving procedures (Fig.2), it was possible to assess complementary mechanical and chemical stability information of the samples (Blaud et al., 2017). Mechanical vulnerability can be assessed by changes in particle size distribution and on the nature of the particles and cement products; chemical mobility can be inferred, in an indirect way, by the presence and relative abundance of specific minerals in the different granulometric classes, including the saline products. Fine particles and salts are very critical due to their high superficial specific area and reactivity (Gupta et al., 2008).

The stability of the soil aggregates is an important feature and has a direct impact on the pore size distribution and consequently on air- water retention and on the soil mobility itself, which in turn affects soil quality (Oades, 1993). Therefore, a comparative analysis considering relative ratios between fractions in DS and WS was done. The WS <0.075 mm/ DS <0.075 mm ratio analysis (S1-19.2; S2-17.6; S3-3.9; S4-7.9; S5-7.4; S6-11.4) showed that, as expected, all values are much higher than 1 (situation where no changes occur). S3 present the lowest value, which indicates that in this deposition place, the surficial materials are relatively loose. In opposition, S1 has the highest value, followed very closely by S2. The enormous difference inside the sedimentation deposit area may be explained by local observations (S2 is in a central and more stable position whereas S3 is in a lateral and well drained location of the flooded area; see Fig. S1 in supplementary material). Similarly, DS >0.85 mm/ WS >0.85 mm (S1-2.2; S2-2.4; S3-1; S4-2.9; S5-2.1; S6-2.8) or DS >2 mm/ WS >2 mm (S1-2.5; S2-1.3; S3-1.3; S4-2.2; S5-2.8; S6-3.8) ratios, e.g., can be used as physical-mechanical vulnerability indicators, giving information about coarser classes behavior under hydrologic regime changes. From the last ratio analysis,

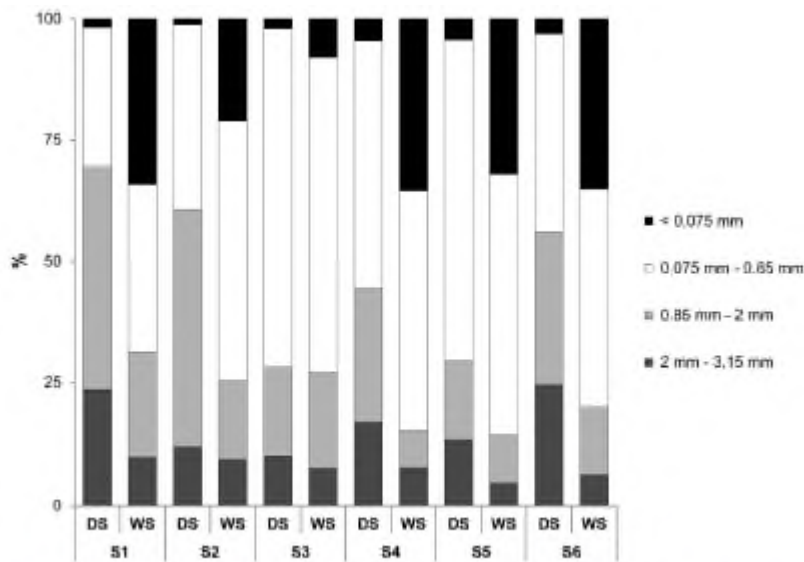


Fig. 2. Granulometric distribution of the São Domingos surface layer (0-15 cm depth) samples (S1 to S6) upon dry sieving (DS) and manual washing and sieving (WS).

we can conclude that big particles (>2 mm) are relatively loose in samples S2 and S3 (the ratio is only 1.3 for both samples). For the remaining cases, more cemented, aggregated or impregnated coarse particles should be present. Once in contact with water, composite earthy clods will tend to separate into smaller and more compact particles. Combining both ratios information (WS <0.075 mm/ DS <0.075 mm or DS >0.85 mm/ WS >0.85 mm or DS >2 mm/ WS >2 mm), it is possible to conclude that S2 and S3 textures are strongly dependent of the hydraulic position inside the depositional basin. S3 is positioned in a peripheral and more washed position, adjacent to a local runoff waterline, whereas S2 is positioned in the center and more stable position.

In summary, both disaggregation and concomitant appearance of fine particles, suggest a very high vulnerability of some of the materials under study, especially if they are submitted to local torrential regime, as is the case for the São Domingos area (IPMA, 2020). In fact, this can be very critical for sediment transport and contamination transfer and dispersion EPA (1990). Results also demonstrate that these samples tend to aggregate themselves in a dry environment, constituting clods or more compact layers, dispersing in the presence of water and mechanical erosion, such as the one promoted by weathering. However, the existent local differences must be considered to optimize field regeneration. Topographic features and runoff waterlines locally control the accumulation/dispersion of soils/sediments and natural biota propagation (Fig. 5), as can be seen in the dam area (see supplementary material Fig. S1).

What is more important in this division of the initial sample is that instead of a global result, an overall average result for each sample, with little discrimination, detailed information about the different sites of the São Domingos area had been obtained. This may help to understand the nature of the problems and mechanisms present in each location, and, therefore, help finding the best responses to overcome them. In this research case study, e.g., the relative amount of salts and their nature also provides valuable information for revegetation purposes.

Fig. 3 shows the granulometric distribution curves of samples (S1 to S6), upon WS and the respective particle size ranges and classification, established in 2002 by the International Organization for Standardization, ISO 14688-1, (Kulhawy and Chen, 2009). As can be seen, in general, it is possible to infer that all disaggregated samples have a coarse texture, given its higher sand and gravel content (between 65% and 68%, for S1, S4, S5 and S6; 79% for S2; and 92% for S3). By considering the physiographic position of the samples, the AMD discharge and the intermediate areas seem to be more powdery (higher silt-clay fractions) with rocky substrate, and the depositional areas are sand/gravel dominant, thus more permeable at surface. As can be seen in Section 3.1.2, these differences can justify the main mineralogical and chemical results found in the studied samples.

Fig. 4 illustrates the stereomicroscopy observations resultant from the WS of S2 (the other samples results are provided in supplementary material, Figs. S2 to S6). The stereomicroscopy observations showed that the overall constitution of the coarser fractions comprises mainly fragments of country rocks with a slightly increase of quartz in silt class. Moreover, the fractions >0.025 mm are mainly composed of rocky fragments (phyllite, quartz veins and metavolcanics country rocks). Ultrafine fraction (<0.025 mm) includes neoformation minerals, related to AMD contamination and rock weathered products, including clays and soluble salts, visible as efflorescences.

In general, with the stereomicroscopy observations it was possible to recognize that all samples have a predominant sandy texture and lithic (phyllite, quartzite and volcanic country rocks) composition. Quartz, and subordinate feldspars, enrichment is also detected in the coarse silt fraction. Even in the ultrafine fraction (<0.025 mm) lithics, quartz and feldspar particles are abundant. Although there are some industrial wastes dispersed in the sites under study, no sulfide ores or metallurgical residues were found in the collected samples. Orange to brownish red fragments were very common in all samples except in S5 (see supplementary material Fig. S5), where gray brittle fragments are the dominant ones. Most part of these colored fragments seems to be weathered regional country rocks. A few plant fragments, probably transported by local water lines from adjacent areas (see supplementary material Fig. S1, were also present in S2 and S3. The images corresponding to the evaporated salts (at the bottom of the images set in Fig. 4 and Figs. S2 to S6 of the supplementary material), enabled the identification of the most mobile elements in each sample. These results confirm the field observations (especially in S2 and S3 sites).

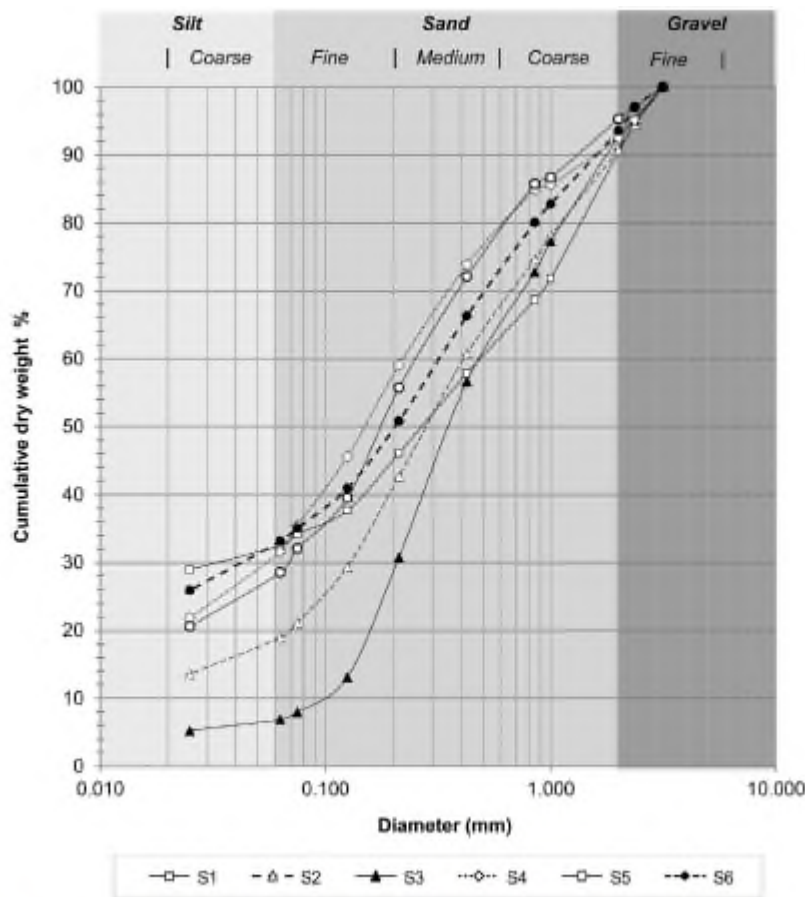


Fig. 3. Granulometric distribution curve of the São Domingos surface layer (0–15 cm depth) samples (S1 to S6) upon manual washing and sieving and the respective particle size ranges and classification according to the International Organization for Standardization (ISO 14688-1; Kulharwy and Chen, 2009).

3.1.2. Mineral and chemical analysis

The XRD results from DS samples with diameter <0.075 mm and from WS samples with diameter <0.025 mm, as well as the leached and further precipitated soluble salts resultant from this separation process, are summarized in Table 1 (the XRD patterns are presented in supplementary material Figs. S7 to S10). For DS <0.075 mm fractions, jarosite group minerals (JGM) are the only detected products related to AMD. Quartz, clay minerals (illite and/or chlorite) and feldspars (typical albite) are present in all samples but in different proportions. There are differences in XRD patterns suggesting the existence of natrojarosite, Nj, $[\text{NaFe}^{3+}(\text{SO}_4)_2(\text{OH})_6]$, and/or hydronium jarosite, Hj, $[(\text{K},\text{H}_3\text{O})\text{Fe}^{3+}(\text{SO}_4)_2(\text{OH})_6]$ and/or other jarosite, $[\text{KFe}_3(\text{SO}_4)_2(\text{OH})_6]$, isostructural phases from JGM. According to the results, S1 and S2 have the lowest proportion of jarosites (Hj), whereas S5 (Nj) and S6 (Hj) show the highest values. S3 (Nj) and S4 (Nj) present intermediate results.

Regarding the WS of the >1 mm fractions (Fig. 4A and B, and Table 1), only samples S2, S3, S5 and S6 presented jarosite group minerals, JGM, with a maximum prevalence in S5. Coarse lithic fragments of samples S1 and S4 do not appear to be contaminated by AMD. In the <0.025 mm class, all the samples have a significant amount of jarosites, coexisting with quartz and minor albite and/or clay minerals (illite and kaolinite (only in S5 sample)). XRD patterns identification for JGM from <0.025 mm class have differences when compared to jarosites from >1 mm class.

Calcium sulfates, with different hydration states (gypsum, bassanite, anhydrite), are the main saline precipitated phases (Table 1). A slight proportion of JGM were also detected in all these fractions but it can be attributed to separation process inefficiency. The same uncertainty about the nature of JGM species was observed in the soluble fraction products. Halite was detected only outside the sedimentary deposits (S2 and S3). On the contrary, aluminum salts (alunogen and tamarugite; see supplementary material Fig. S11), and rozenite (iron sulfate hydrate salt) are restricted to the sedimentary deposits, as well as minor calcite. Dissolution and hydrolysis of aluminosilicate minerals from outcrop rocks should be the source of this highly soluble aluminum salts, usually occurring in efflorescence's and capillary films as a result of evaporation (Long et al., 1992; Murray et al., 2014).

The S2 yellowish and grayish saline crusts (1–2 cm thickness top layer) manually separated from a bulk sample, presented up to 50% (w/w) of soluble fractions that were also analyzed by XRD. Alunogen $[\text{Al}_2(\text{SO}_4)_3 \cdot 16\text{H}_2\text{O}]$, copiapite $[\text{Fe}_{14}\text{O}_3(\text{SO}_4)_{18} \cdot 63\text{H}_2\text{O}]$, scorodite $[\text{FeAsO}_4 \cdot 2\text{H}_2\text{O}]$ and an unnamed mineral $[\text{Al}_3(\text{SO}_4)_2(\text{OH})_5 \cdot 9\text{H}_2\text{O}]$ were found in the yellowish crusts. Nj, alunogen,

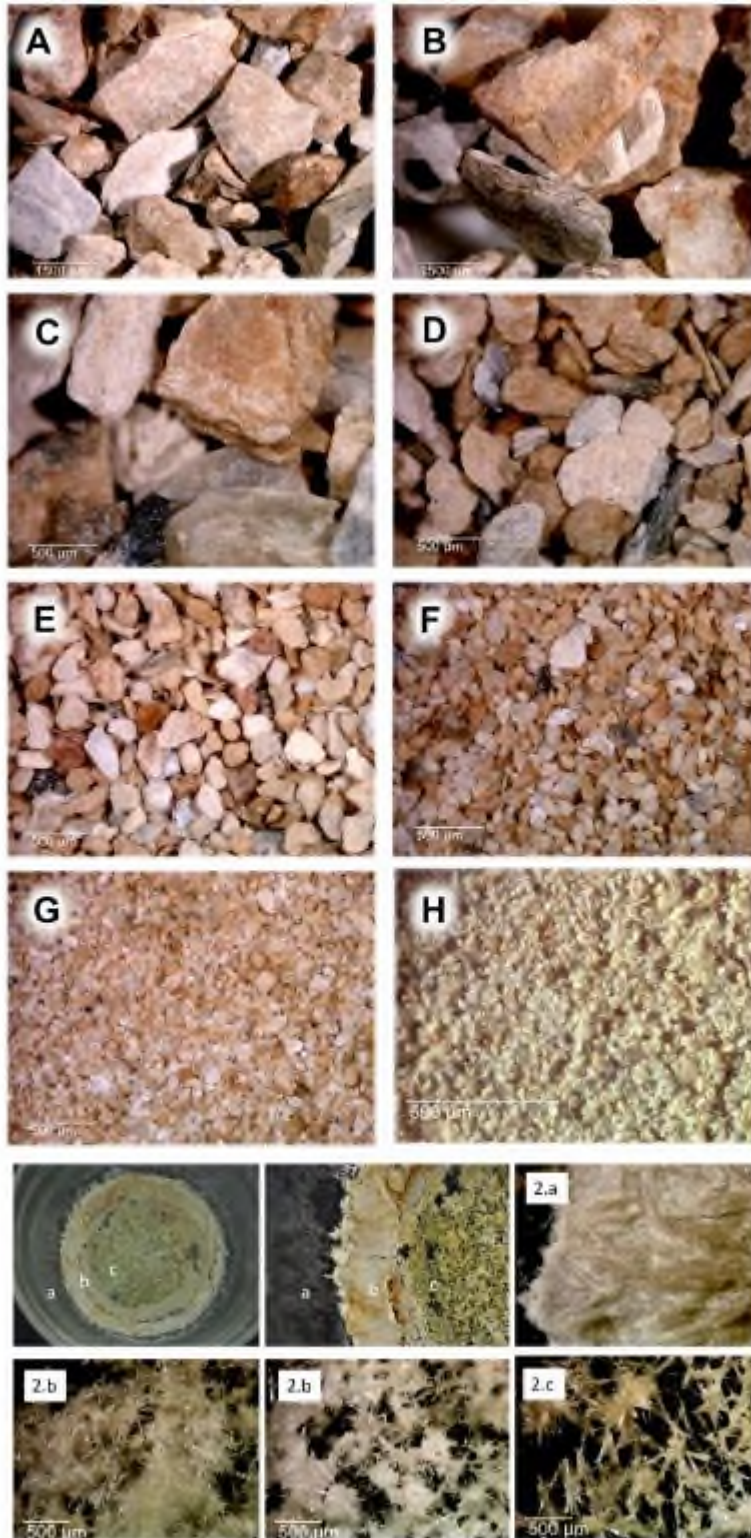


Fig. 4. Stereomicroscopy observations of the manual washing and sieving products from S2 (A to H; clasts 3.15–2.36, 2.36–1, 1–0.425, 0.425–0.212, 0.212–0.125, 0.125–0.063, 0.063–0.025 and <0.025 mm), lower set of 6 pictures depicts the resultant precipitated soluble salt fractions (a, b and c), after drying the washing water at 30 °C.

Table 1
Mineralogical composition (analyzed by XRD) of the São Domingos surface layer (0–15 cm depth) samples (S1 to S6) <3.15 mm, upon dry sieving (DS) and gentle washing sieving (WS) and the resultant precipitated soluble salts, after drying the washing water at 30 °C. Mineral species are cited by relative abundance order (relative intensity of XRD reflections and pattern scores). Jarosites are indicated in bold. Granulometric fractions (dry weight %) are indicated between brackets.

Sample ID	DS		WS		Soluble cations*
	<0.075 mm	3.15–1 mm	<0.025 mm	Salts	
S1 Acid drainage leached rock outcrop	Qt, Il, Ab, Hj, Cl (1.8)	Qt, Ab, Il (28.2)	Qt, J, Il (29.0)	Cy, Hal, J (0.1)	Ca, Na, K
S2 Acid drainage sediment deposit	Qt, Ab, Il, Hj (1.2)	Qt, Ab, Il, Nj (21.5)	Qt, Nj, Ab, Il (14.6)	Cy, Bas, Anh, Cr, Nj, Ros, Tam, Akt (1.2)	Ca, Na, K, Al, Fe
S3 Acid drainage sediment deposit	Qt, Ab, Nj, Il (2.0)	Qt, Ab, Il, Hj, Hal (22.6)	Qt, Nj, Ab, Il (6.1)	Cy, Nj, Tam (0.9)	Ca, Na, K, Al
S4 Acid drainage leached mine tailings deposition	Qt, Il, Nj, Ab (4.5)	Qt, Ab, Il (14.3)	Qt, Hj, Ab, Il (22.3)	Cy, Hal, Nj, J (0.6)	Ca, Na, K
S5 Acid drainage leached rock outcrop	Qt, Nj, Msc, Ab (4.3)	Qt, Nj, Ab, Il (13.3)	Qt, Nj, Ab, Il, Kao (20.7)	Cy, Bas, Hal, Nj, Mg–S (0.2)	Ca, Na, K, Mg
S6 Acid drainage superficial deposition	Qt, Hj, Il, Ab, Mic (3.1)	Qt, Il, J, Ab (17.2)	Qt, Hj, Il (26.1)	Cy, Bas, Hal, J (0.3)	Ca, Na, K

Notes: * Soluble cations were inferred according to the precipitated salts. Ab-Albite (NaAlSi₃O₈); Alu-Alunogen (Al₂(SO₄)₃·16H₂O); Anh-Anhydrite (CaSO₄); Bas-Bassanite (CaSO₄·0.5H₂O); Cr-Calcite (CaCO₃); Cl-Clinoclrite ((Mg,Al)₂(Si,Al)₄O₁₀(OH)₂); Cy-Gypsum (CaSO₄·2H₂O); Hal-Halite (NaCl); Hal-Hallauite (Al₂Si₂O₇(OH)₄); Hj-4hydronium-jarosite ((K,H₃O)⁺[SO₄]₂(OH)₆); Il-Ilite ((K,H₃O)Al₂Si₂AlO₁₀(OH)₂); J-Jarosite (KFe₃(SO₄)₂(OH)₆); Kao-Kaolinite (Al₂Si₂O₅(OH)₄); Mg–S—Magnesium sulphate hydrate (MgSO₄(H₂O)₆); Mic-Microcline (KAlSi₃O₈); Msc-Muscovite (KAl₃(AlSi₃O₁₀)(F,OH)₂); Nj-Natrojarosite (NaFe₃(SO₄)₂(OH)₆); Qt-Quartz (SiO₂); Ros-Rosenite (FeSO₄·4H₂O); Tam-Tamarugite (NaAl(SO₄)₂·6H₂O).

gypsum [CaSO₄·2H₂O] and sarmientite [Fe₂(AsO₄)(SO₄)OH·5H₂O] were found in the grayish crusts. Results indicate that the real evaporitic paragenesis in this location is more complex, but Al and Fe sulfates are dominant. The novelty is the presence of Fe arsenate or sulfate-arsenate (even though their relative abundance is limited) together with copiapite. Besides the high acidity generated by soluble iron and aluminum sulfates, due to Fe and Al hydrolysis (Sánchez España et al., 2005; Dold, 2014), the occurrence of soluble arsenian compounds can also constitute an environmental concern regarding water contamination and plants development and survival, even for the more adapted ones as *Erica andevalensis*, *Erica australis* and *Cistus ladanifer* (Abreu et al., 2008; Abreu et al., 2012; Santos et al., 2016).

Considering the results of XRD analysis, it was not possible to positively identify the existence of an eventual toxicity by metal or metalloids in the analyzed locations, because there was not found any anomalous specific mineralogy. Only very limited occurrence of arsenate or sulfate-arsenate were identified. Even with this limitation, it was possible to infer the existence of potential harmful concentrations related to local abundance of JGM. In fact, a strong correlation between jarosite abundance and metal(loid) concentration was found in chemical data, as can be seen further in this section. Widespread jarosite (1 to 15% wt), as well as goethite and hematite occurrences in São Domingos mining area are related to several mining waste sources (Matos et al., 2006), with jarosite being seen as the most stable sulfate mineral. For this reason, chemical and mineralogical detailed studies of São Domingos highly contaminated areas are essential to the knowledge of the dynamic processes that govern the release, transport, retention and probable later remobilization of free-metals after sulphide-oxidation (Sánchez España et al., 2005; Álvarez-Valero et al., 2008; Pérez-López et al., 2008; Chou et al., 2013).

Otherwise, the existence of the jarosite mineral group is considered as an efficient positive environmental contribution to metal and metal (loid)s sequestering (Figueiredo and da Silva, 2011; Murray et al., 2014; Cogram, 2018; Fall, 2019). As pointed out by Figueiredo and da Silva (2011), which studied in detail AMD jarosite rich depositions in Achada do Gamo region (silty grayish material rich in Ca, Ti, As and Pb, with minor K, Se, Sb and Bi), jarosites make retention of Pb, and possibly other metals. A preliminary SEM-EDS study (MicroLab-IST) from a S2 jarosite bearing fraction enable us to confirm the existence of an unusual Cu bearing Nj as euhedral pseudo cubic crystals with a 2-micron side. This result may indicate that local geological-chemical differences, in association with distinct AMD processes, can generate different mineral species from the alunite-jarosite supergroup, being capable of sequestering elements with average to big size, as indicated by Figueiredo and da Silva (2011). This aspect is very relevant because if the metals are sequestered in a more stable crystalline structure, even at high concentration, the critical elements may not be bioavailable.

Channel discharges of acidic wastewater ended around 54 years ago. Since then, AMD is becoming less expressive, and mechanical erosional processes are controlling jarosites removal from the strongly weathered and contaminated rocky slopes, and further downstream transport and accumulation. This way, at least two generations of jarosites could coexist at present time near the dam deposit, detrital facies typical from proximal rocky regions, and an authigenic facies growing in the seasonal flooded area. This aspect may be related to the variability of XRD patterns found in the studied jarosites. This situation was already reported in another AMD sulfide related system (Dold, 2014; Murray et al., 2014; Fall, 2019). A detailed study on the minerals of the jarosite group (Long et al., 1992; Desborough et al., 2010; Scarlett et al., 2012; Dold, 2014; Cogram, 2018) is beyond the scope of this study but is a key issue in future geochemical studies for the São Domingos area.

Moreover, it has been reported that, in natural acidic environments, the biogenic formation of jarosite, generally associated with bacterial activity, may also be due to acidophilic fungi (e.g., the fungal strain isolated from Rio Tinto *Purpureocillium lilacinum* specifically precipitates Hj (Oggerin et al., 2014)). Thus, the comprehension of the adaptive mechanisms of microorganisms that prosper in this severe environment might allow us to better assess the possible ecological effects of environmental changes.

Oxidative and low pH (around 2; Table 2) still found in the flooded area (S2 and S3 locations) could represent the ideal conditions for jarosites formation even at the present time (Sánchez España et al., 2005; Álvarez-Valero et al., 2008; Pérez-López et al., 2008; Dold, 2014; Fall, 2019). The same conditions can be predicted for the wastewater discharges that occurred in the past along the slopes of the São Domingos valley stream.

Table 2
Physico-chemical properties of São Domingos surface layer (0–15 cm depth) samples (S1 to S6), evaluated in the <2 mm dry sieved fraction. Values are a mean of three independent determinations ± stdev.

	S1	S2	S3	S4	S5	S6
pH (H ₂ O)	3.6 ± 0.0	2.1 ± 0.0	2.3 ± 0.0	3.2 ± 0.1	3.9 ± 0.1	3.5 ± 0.1
M (%)	5.5 ± 0.0	4.3 ± 0.3	3.7 ± 0.3	3.8 ± 0.1	2.0 ± 0.2	2.4 ± 0.2
LOI (%)	2.9 ± 0.2	2.3 ± 0.1	2.6 ± 0.2	3.2 ± 0.2	2.7 ± 0.2	2.3 ± 0.1
EC (dS m ⁻¹)	0.37 ± 0.01	4.97 ± 0.08	3.48 ± 0.05	0.66 ± 0.01	0.11 ± 0.00	0.46 ± 0.04

Note: Electrical conductivity (EC); moisture content (M); loss on ignition (LOI) at 450 °C.

Additionally, and as can be seen in Table 1, S2 has the most complex composition, with different sulfates of Ca, Al and Fe, whereas the S5 has a residual quantity of a magnesium sulfate hydrate (PDF 00-020-0690). By considering the weight of the soluble fractions in the different samples it was possible to distinguish the sedimentary depositional area from the other ones (Table 1). Moreover, the amount and the nature of the salts accumulated in this basin could be critical for revegetation purposes due to the high salinity and aluminous composition (Bojórquez-Quintal et al., 2017).

The results from the WS precipitated soluble salts (Table 1) and from the ones obtained from the EC for <2 mm fraction are in agreement (Table 2). The EC results for the leached rocks samples (S1 and S5) were very low whereas the sedimentary deposit samples (S2 and S3) presented very high values. The results of pH and EC for <0.075 mm fractions concur with the chemical results. The fine powders from leached rocks (S1 and S5) are less acidic and have fewer dissolved salts. The samples from the sedimentary deposit have a pH of around 2 and present an enormous quantity of dissolved salts (max. around 5 dS m⁻¹). As said before, S3 is in a more drained area than S2, and presents a less slightly acidic behavior and less dissolved salts (3.5 dS m⁻¹). This result is in accordance with the textural analysis results (Section 3.1.1). S4 and S6 samples have intermediate values.

The pH of outcrop rock samples collected in the S1 location (S1RA, a creamy yellow color rock, with minor jarosite, and S1RB, a reddish orange color rock, with minor jarosite only in the more weathered parts; see Fig. 5) is higher in comparison to the superficial sample S1 (pH ≈ 3.6; Table 2). S1RA has pH value around 4.5 (both compact rock and small fragments) and S1RB has pH value around 6.7 (both compact rock and small fragments). The precipitated salts from S1RA are calcium

sulfates and halite while in S1RB additional sylvite and jarosite were identified. These results clearly show that the location is undergoing a process of natural regeneration, evidenced by scattered moss, young *Cistus* plants and small roots (Fig. 5), namely in the better drained or more physiographical stable areas.

Salt and fine products composition and abundance enabled us to define an overall dichotomy between the proximal/discharge superficial AMD areas and distal/sedimentation superficial areas. The former is enriched with JGM and the last presents an acidic and hypersaline tendency. Thus, the revegetation strategy to be applied in each location must consider these differentiating aspects. As was previously mentioned (Section 3.1.1) the comparison between WS and DS samples anticipated a dichotomy in the chemical typology of the samples. Therefore, the combination of the DS and the WS can bring important additional information for forecasting results and/or preparing sustainable decontamination and revegetation projects. The importance of the granulometric characterization is also well-evidenced in the work of EPA (1990). Also, and because this is a space and a time related problem, other key factors must be taken into consideration.

The composition of samples and the corresponding precipitated salts are of utmost importance for the evaluation of the availability of the elements in the context of the revegetation of the area. The salinity dynamics is also very important since high salinity is one of the main limitations for the revegetation (Dinis et al., 2020) and of the analyzed locations (Tables 1 and 2). A cyclic regime of drought followed by heavy rain episodes is frequent in the São Domingos region (IPMA, 2020). Depositional areas during the dry seasons often create cracks, fine particles aggregation and compaction, and salt efflorescence. Otherwise, in wet seasons, fine particles washout from the top layers, mud transport and salt solubilization were observed. Residual acidic water level is temporarily accumulated at the top of the depositional area near the local dam. The combination of these adverse conditions may be another key factor behind the phytotoxicity of the area (absence of plants).

In fact, the relation between salinity and mineral nutrition of plants is particularly intricate. Grattan and Grieve (1998) stated that the salinity-induced nutritional disorders might “result from the effect of salinity on nutrient availability, competitive uptake, transport or partitioning within the plant”.

The LOI values obtained are relatively high and similar (between 2.3 and 3.2; Table 2) and should mainly reflect the amount of secondary minerals, especially sulphates and clay minerals that decompose totally or partially up to a temperature of 450 °C (Pansu and Gautheyrou, 2006). A substantial part of this mass loss must be related to the dehydrolyzation of jarosites (around 10% loss mass), which is practically complete for most of the minerals in the alunite-jarosite group at 450 °C (Kerolli-Mustafa et al., 2016). The additional presence of compounds with the radical (OH)⁻ or kaolinite in S2, S3 and S5 samples can explain the observed highest values. Hence, a direct correlation between the LOI and organic matter content should not be done. In fact, the samples organic matter content is expected to be very low. Total organic carbon measurement should have been a more suitable methodology to clarify this aspect.

The chemical elements concentration in <0.075 mm DS fractions of São Domingos samples is resumed in Table 3. Elements with systematical low values in all the samples are also indicated (see notes of Table 3). To check the sample's possible anomalous character in a more realistic (weighting) way, simultaneous analysis of the chemical content and weight of granulometric class to the total sample (Table 3) should be done. Moreover, the combination of these parameters enables an indirect estimation of absolute element content value and comparison between samples. The use of a gray shading in Table 3 facilitates a quick comparative fuzzy reading of the samples (considering 3 classes for each element). The highest values are indicated in dark gray and the lowest in light gray. The median values are not highlighted.

Considering that the fine fraction of the DS (<0.075 mm) is the one that potentially contributes the most to the concentration of hazardous elements, it can be depicted from Table 3 that the weight values are considerably different from each other, using the original sample or only the fractions <3.15 mm. The S2, S3 and S5 samples show small differences in <0.075 mm fractions (original versus after >3.15 mm removal fraction) whereas, on the remaining samples, the values almost double. This is due to the gravel content of these samples, that is very low in S2, S3 and S5 and very significant in S1, S4 and S6. Overall, it's possible to infer that S4, S5 and S6 samples produce more fine fractions upon DS, and also by WS (but in that case, including S1). Given the fact that the gravel fractions are potentially the least contaminated with hazardous elements, the focus of our results analysis will be the <3.15 mm fractions. Finally, the interpretation of chemical results attend not only these aspects but also to the textural analysis upon WS.

S1 has a small percentage of <0.075 mm DS fraction (1.78%) with a relative high content of P, Li, Mg, Ca, Al, V, Cr, Mn, Ni, Cu, As and Ba (Table 3). The content of S, Na and Pb are the least of the sample set. The overall composition reflects the nature of the fine phyllite substrate particles combined with remnants of AMD. WS results highlighted the cloddy structure of the sandy fraction; hence, the percentage of fine particles was undervalued and its metal(loid) content is not negligible.

The S2 and S3 have an average composition for the utmost part of the elements, except for K, As, Sn, Sb, and Hg that are relatively depleted whereas S, Fe and Na, Mg, Al, or Sr are comparatively higher (Table 3). These anomalous values can be attributed to a significant presence of jarosite combined with soluble salts, as showed by the XRD analysis (Table 1 and see supplementary material Figs. S7 to S10). Results reinforce the idea that top layers from depositional area are hazardous metal (loid)s depleted. As S2 and S3 samples, S4 is also S and Fe rich, but in this case higher values of Hg, Pb, Bi and Se were registered (Table 3). In this case, these values could be very critical since <0.075 mm fraction reaches almost 4.5% of the DS sample, and WS results are also very high. Local sedimentation accumulation controlled by tailings impoundment could justify the high absolute amount of hazardous metal(loid)s in this site. S5 has one of the biggest percentages on the <0.075 mm fraction (4.33%; Table 3). The presence of illite and kaolinite clays makes this sample very friable. Low values of S and base metal (Fe, Cu, Zn, Pb),

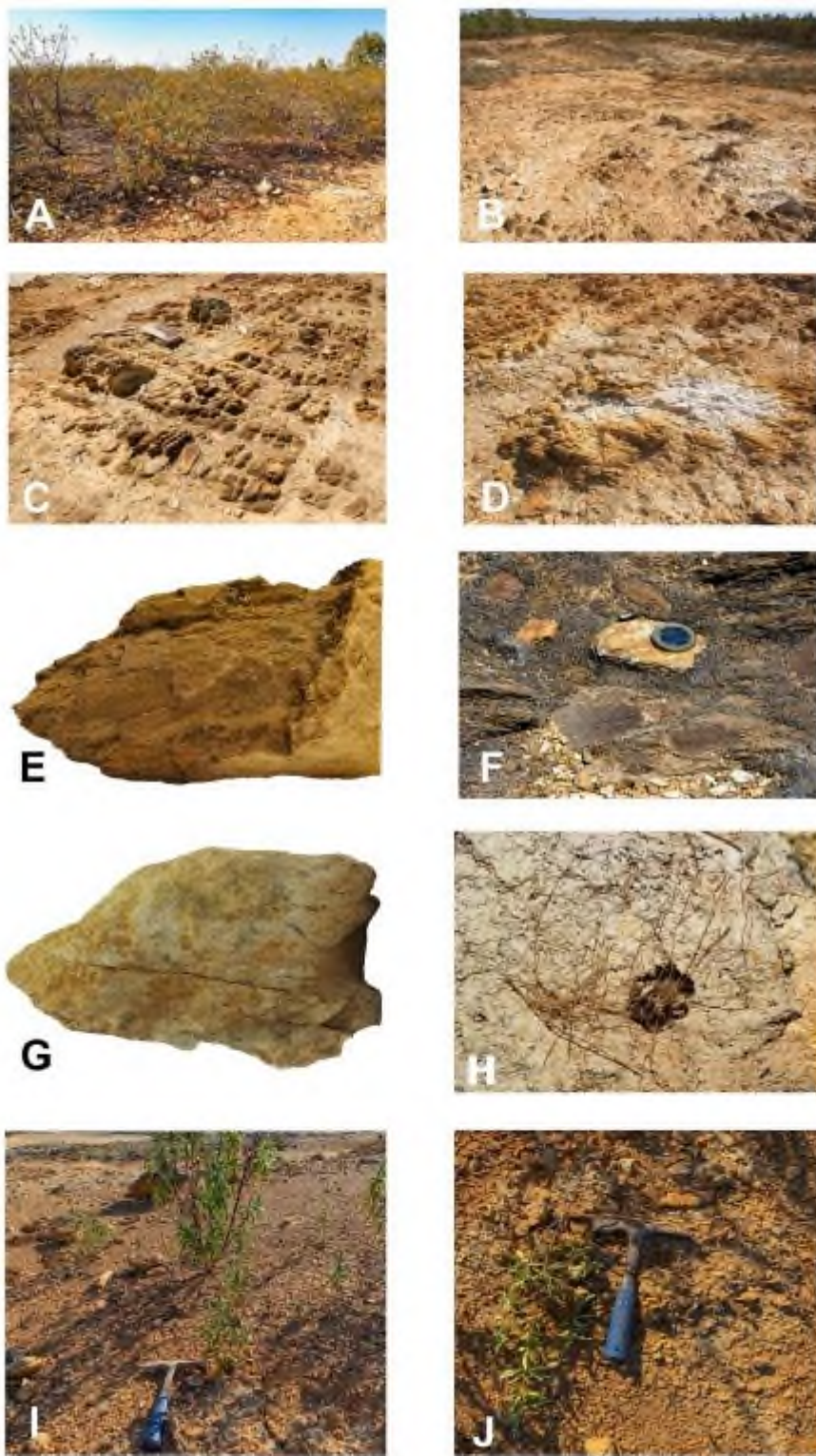


Fig. 5. Outcrop rocks from site S1 (proximal/discharge area). A - Autochthonous species in AMD transition zone; B to D - Evidence of strong AMD weathering and impregnation; E - S1RA sample; G - S1RB sample; Evidences of the undergoing natural regeneration: F - mosses, H - small plant roots and animals, I - young *Cistus* plants J - detail of *Cistus* roots morphology (showing parallel to surface development).

among other metals, indicate low contamination related to AMD, but high content of Nj is found in DS and WS fractions. On the other hand, high relative content of As, Sn, Sb, Tl, Hg points to a primary concentration of these metals in the substrate. So, overlapping of chemical signatures (AMD and lithological) could be present in this site; therefore, the values of some of these elements may not be negligible. S6 compositional profile indicates a location related to AMD drainage contamination, and presents the highest concentrations for Hg, Pb, Cu, Zn and Bi, and the lowest cumulative value of nutrient elements (P, Ca, Mg, Na). Taking into account these results, and the mineralogical composition of DS and WS fractions, the hazardous metal(loid)s absolute values should not be negligible. Potential critical issues for plant growth and survival seem to be present in this site.

Arsenic was found in close association in rock outcrops deposits. Hence, As can be found primarily in rock substrates or can be trapped in proximal areas of AMD via jarosite precipitation. The superficial layers of AMD sedimentary deposits (S2 and S3) are relatively depleted of toxic metals but reveal a high concentration of soluble sulfates (see XRD of WS < 0.075 mm fractions and soluble fractions/salt analysis, Table 1 and supplementary material Figs. S7 to S10). This fact can be problematic for natural revegetation. On the other hand, Pb (alongside with Hg, As, Cu, Zn) concentrations found in S4 and S6 can be critical due to its combined toxicity.

The chemical composition results combined with the image analysis of sieved wet fractions (Fig. 4 and supplementary material Figs. S2 to S6) and the XRD analyses (Table 1) indicate that the overall trace elements anomalies are mainly dependent on the jarosite existent in the fine fractions and soluble salts.

Soil quality regulation, like the Ontario Environmental Protection Act (Government-of-Ontario, 2011), set up recommended standards limit values for several soil uses, using <2 mm DS sample fractions. In our analysis the <0.075 mm DS was used so, it is not possible to do a direct comparison of values. Even knowing that the real values for the critical metals and metal(loid)s in <2 mm fraction should be lower than the values presented in Table 3, and that WS <0.075 mm (including dissolved salts) and DS <0.075 mm have similar composition, two approaches can be done: (1) by considering that all the remnant DS fractions do not contribute to sample concentration of hazardous metal(loid)s, which is a very underestimated approach; (2) by using the WS <0.075 mm fraction combined with DS <0.075 mm chemical results, assuming that the remnant WS fractions do not contribute to sample concentration of hazardous metal(loid)s, as was demonstrated by stereomicroscopy observations and XRD analysis.

Using the first approach, and comparing the obtained values (see supplementary material Table S1) with the recommended standards limit value for parkland as established by the Ontario Environmental Protection Act (Government-of-Ontario, 2011), we can infer that the studied locations are not highly metal(loid) contaminated. The data analysis revealed that the most problematic elements are As, Hg and Sb, and that these occur, mainly, in the S5 location. This assessment also indicates that S6 is highly contaminated with Hg. The obtained results are in accordance with other authors, especially for the high As and Sb concentrations (Abreu et al., 2008; Anawar et al., 2011; Andr  s et al., 2018; Arenas-Lago et al., 2018). Using the second approach (results not presented), the absolute value of hazardous metal(loid)s present in S1, S4, S5 and S6 sites will be much higher. This multiplicative effect is strongly dependent on the WS <0.075 mm/ DS <0.075 mm ratios, that can reach very high values (e.g. almost 20 in S1 sample); that way, besides the previously indicate hazardous elements, other elements, as Cu, Zn, etc., could be critical for the remediation or revegetation plans.

As previously mentioned, although some of the levels of the critical elements for the development of plants could indicate potential anomalous trends in the studied samples, the nature of the phases carrying those elements is decisive to determine the possible toxicity of the studied selected sites. Considering the JGM as the main sequestering phases of the most dangerous metal(oid)s, their stability in the context of physical, chemical and biological processes will be of extreme importance for remediation or revegetation programs since they control metal(loid)s bioavailability.

3.2. Soil quality assessment

BGL, AS and DH enzymatic activities were not detected in S  o Domingos soil samples (see supplementary material Table S2). Surprisingly, APM activity was quantifiable in all samples ranging from $201 \pm 4.1 \mu\text{g pNP g}^{-1}_{\text{soil}} \text{dw h}^{-1}$ for S4 down to $18.8 \pm 1.2 \mu\text{g pNP g}^{-1}_{\text{soil}} \text{dw h}^{-1}$ for S6.

The measurement of soil enzymatic activity can function as a good soil quality indicator, once it reflects the microbial presence in the soils. DH is considered to be part of intact living cells and does not accumulate extracellularly (Kaczy  nska et al., 2015). Moreover, the degradation of cellobiose by BGL in soils is due to enzymes excreted by proliferating organisms rather than the accumulated extracellular enzymes (Turner et al., 2002). The absence of both enzymes (DH and BGL) in all the samples may reflect the ecotoxicity of the collected sample and that the microbial population in the mine soil samples might be very low. The presence of the AS enzyme has been correlated with thriving microbial biomass and may persist in the soil associated with organic matter (Whalen and Warman, 1996). Hence, the deficiency in AS activity shows the absence of proliferating microorganisms and the lack of organic matter, on which most microbes depend on. The reported enzymatic activity values are possibly related with previously mentioned soil physicochemical properties (Table 2), such as the acidic pH of the samples. This parameter has proved to be as important as soil carbon and nitrogen concentration in influencing the microbial biomass, not only by affecting nutrient solubility, but also by potentiating metal toxicity (Aciego Pietri and Brookes, 2008). Other possible cause for the absence of enzymatic activity might be related with the samples texture, given that it has been proved that for sandy loam soils the enzymatic activity decline is greater due to more difficult stabilization of organic matter (G  nal et al., 2018).

However, the detection of APM activity does not fit in this explanation. There are several possible interpretations for the disparities registered in the enzymatic assays results. Firstly, the measured APM activity may be influenced by the type of predominant organisms responsible for its secretion. APM is an intra- and extracellular enzyme that is produced not only by microbial populations but also by plant cells, and within the microbial populations that produce this enzyme, fungi are the most common (Orzevska et al., 2012). Adding to this, APM is an inducible enzyme, i.e. the lack of substrate stimulates the enzymatic production (Margesin and Schinner, 1994). The detected activity of this enzyme when compared with the remaining ones may be explained by the fact that fungi are a microbial group that are able to adapt to a wide range of pH, including hyper-acidic pH (Smith and Doran, 1996), combined with the fact that the surroundings of the locations where the samples were taken had vegetation (see Fig. 1 and supplementary material Fig. S1). Moreover, the differentiation between the intra- and extracellular APM in the soil samples was not carried out. Thus, the detected APM activity could also be due to the increase of the total APM in the soil, caused by the release of intracellular APM from the lyses of microbial cell, as a result of the end of their life cycle (Rejsek et al., 2012).

Secondly, the lack of activity for most of the tested enzymes may be related with its physiological availability. Amino acid functional groups are pH sensitive, as they can undergo irreversible conformational and chemical changes upon acidic pH disabling its ability for substrate binding and catalysis (Dick et al., 2000). Despite the optimal pH activity of APM being set between 4.5 and 6.5, other studies suggest that higher activity rates of this enzyme can be seen in soils with $\text{pH} < 4$ (Turner, 2010). Thus, APM may be more resistant to pH fluctuations than the remaining extracellular enzymes. Moreover, the location of the enzyme in the soil matrix can influence its activity. When compared with free in solution enzymes, those that are adsorbed to solid surfaces can undergo

Table 3

Chemical composition of São Domingos surface layer (0–15 cm depth) samples (S1 to S6), evaluated in the <0.075 mm dry sieving fractions and determined based on soil dry weight. For each element 3 relative classes were considered: the dark gray shading indicates the highest values and the light gray the lowest, whereas the median values were not highlighted.

		% < 0.075 mm*	0.94	0.98	1.71	2.29	3.68	1.70	
		% < 0.075 mm**	1.78	1.20	2.03	4.49	4.33	3.08	
Units		DL	S1	S2	S3	S4	S5	S6	
Al	%	0.01	1.74	0.42	0.88	0.49	0.37	0.41	
Ca		0.01	0.04	0.02	0.02	0.01	0.01	< 0.01	
Fe		0.01	3.73	5.03	5.96	6.20	3.64	4.01	
K		0.01	0.31	0.20	0.19	0.29	0.23	0.46	
Mg		0.01	0.32	0.02	0.09	0.02	0.02	0.02	
Na		0.001	0.10	0.33	0.21	0.25	0.25	0.16	
P		0.001	0.03	0.01	0.02	0.02	0.01	0.01	
S		1.00	< 1	2.00	2.00	2.00	3.00	2.00	
Ti		0.001	0.05	0.05	0.05	0.01	0.00	0.01	
Ag		mg kg ⁻¹	0.002	0	2	2	4	0	8
As			0.10	1980	268	435	963	3920	908
Ba			0.50	197	42	50	22	80	20
Bi			0.02	39	15	16	47	12	52
Ce	0.01		42	19	19	28	27	17	
Cr	1.00		22	7	16	11	5	11	
Cu	0.20		235	107	160	180	7	278	
La	0.50		21	11	11	13	14	8	
Li	0.10		18	3	9	5	2	5	
Mn	1.00		106	23	49	17	5	23	
Nd	0.02		15	6	7	11	11	8	
Ni	0.10		11	2	6	3	3	3	
Pb	0.10		404	1636	1340	2726	477	3570	
Rb	0.10		16	9	9	13	9	21	
Sb	0.02		42	31	35	70	206	80	
Se	0.10		10	5	5	11	1	9	
Sn	0.05		10	9	8	8	31	17	
Sr	0.50		33	39	32	34	42	17	
Tl	0.02		14	3	3	11	17	7	
V	1.00	31	16	27	18	8	9		
Zn	0.10	40	38	46	14	16	99		
Zr	0.10	12	7	8	6	5	7		
Au	µg kg ⁻¹	0.50	19	25	26	275	2	82	
Hg		10.0	1610	470	1730	4170	3780	> 10000	

Notes: * Dry weight percentage relative to original sample >3.15 mm. ** Dry weight percentage relative to sample <3.15 mm. Analyzed elements not included in the Table: (a) Above the detection limits and ≤2 mg kg⁻¹ (except for Au and Hg): Be, Cd, Dy, Er, Eu, Gd, Ge, Hf, Ho, In, Lu, Nb, Re, Sm, Ta, Th, Tm, U, W and Yb; (b) Values >2 and ≤5 mg kg⁻¹: Co, Cs, Ga, Pr, Sc, Te, Th and Y; (c) Values >6 and <10 mg kg⁻¹: Be and Mn.

conformational changes that may change its availability and/or change their optimal pH (Turner, 2010). Therefore, results did not allow withdraw conclusions about the microbial communities in the tested São Domingos locations. As stated before, the knowledge of the adaptive mechanisms of microorganisms to prosper in these extreme environments would be of great help in the evaluation of a revegetation and phytoremediation strategy for the studied sites. However, all the gathered information of this study is a step forward in that direction.

4. Conclusions

Our integrated methodological approach, combining fieldwork observations and detailed information about the collected products, enables a better understanding of the nature of the problems and mechanisms present in each of the selected locations subject to AMD in the São Domingos area. In particular, in the place where more samples were taken (S1 to S4) it was possible to develop an integrated study from the geochemical and environmental point of view, which helped us to track the evolutionary path of this region to the present day. Considering a retrospective analysis, it appears that the AMD area of this small hydrographic basin is relatively stabilized at the surface, from the point of view of the dispersion of metal(loid) contamination towards the São Domingos stream. Field observations disclosed that the section of the waterline after the dam, and in the continuity of the sedimentary flood deposit, despite having no vegetation, only presented a limited presence of salts and colorations, spread in just over a dozen meters.

The combined use of wet sieving and dry sieving was a very important aspect for obtaining relevant information for the on-going evaluation. Results suggest that the materials under study, subjected to local torrential hydrologic regime, have high mechanical vulnerability, critical for erosion, mud transport, and contamination transfer and propagation, critical for plant root and microbial communities' establishment.

Two main criteria, nature and fraction of soluble phases (e.g. conditioning EC and pH), and the chemistry of surficial products (e.g. metal and metalloids) related to jarosite presence, enable us to set up an overall dichotomy between superficial proximal/discharge and distal/sedimentation areas. Even though wastewaters and geological substrates can be different from place to place in the studied locations, a strong dependency on physiographic, hydrologic and climatic factors is found. Nowadays, the old wastewater discharge areas, located on the slopes of the São Domingos stream valley, are enriched in the JGM. On the other hand, the surficial products from the flooded dam area are very acidic and hypersaline aluminous. The decreasing concentration of metals and metalloids from the proximal to the most distal regions is mainly related to the presence of jarosite, since other secondary minerals, as iron oxides and hydroxides, only exist in very limited concentrations. Due to natural erosional processes we believe that this gradient between proximal and distal regions should have been higher in the past. The iron and sulfate acidic waters rapid evaporation, when in contact with regional country rocks, could largely favor jarosites formation. In that way, JGM provided an efficient positive environmental contribution to metals and metalloids sequestration/immobilization and subsequent deposition and/or local accumulation.

As, Pb, Sb and Hg seem to be the more critical elements in the studied samples. However, and since these elements seems to be sequestered mainly by JGM, their bioavailability should be very limited.

Channel discharges of acidic wastewater ended around 54 years ago. Since then, AMD is becoming less obvious. Mechanical erosional processes are controlling jarosites removal from the strongly weathered and contaminated rocky slopes, as well as their further transport and accumulation downstream. At least two generations

of jarosites could coexist at present time near the dam deposit, detrital facies typical from proximal regions, and an authigenic facies growing in the seasonal flooded area.

The local presence of species from the native flora, e.g., in runoff waterlines or in permeable gravel deposits, clearly shows that some locations are undergoing natural regeneration. That is the case of outcrop rocks at site S1, as could be seen by physical and chemical parameters.

Low toxicity and ecosystem regeneration evidences, observed in surficial levels of proximal or intermediate areas, suggest that revegetation plans can be achieved in a short time, by providing a stable and sustainable physical structure (macropores, and natural or artificial water-stable aggregates, etc.), and using well adapted autochthonous plants. Macro fissuring and permeable infillings can help hydraulic (water infiltration), physicochemical processes (ion adsorption/desorption, oxidation/reduction conditions, pH, ions solubility) necessary to restore, foster and stimulate biological activity in the plant's root zone.

According to our results, regeneration-revegetation of AMD distal sedimentation deposits is more challenging due the intrinsic abiotic constraints present in the accumulated and diagenetic evolved materials, including a dysfunctional physical structure and hydraulic capacity. The different areas present high salinity and permeability on the alluvial top layer, which showed high geochemical variability. Indeed, seasonal rain and runoff events, high soluble content of Fe and Al salts and its high acidity, the easy phase transition (des)hydration and release or precipitation of metal(loid)s in sequestering phases, and the sorption processes therein, influence the cyclical availability or retention of the hazardous elements. Alunogen is by far the most common salt, which makes this place particularly toxic for plants. Al and Fe soluble sulfate crusts are also responsible for high acidity and low pH (<2). In this case, the execution of an in-depth soil profile should be considered, to determine the deposit's dimension and structure, and the deep layers biological viability (since jarosites can become a problem, due to their potential breaking down and possible release of sulfate and hydrogen ions, as well as sequestered trace metals and other contaminants). If very toxic conditions are found the system should be isolated with the available overburden materials, prior to use natural or artificial topsoil. Removal of secondary minerals from their stability region or creating contact with different types of materials can generate unexpected and very problematic sources of acidity.

Better vulnerability studies and more adapted risk maps can be designed based on this AMD impact assessment research to allow for the selection and establishment of a sustainable phytoremediation strategy for the São Domingos mine area or other equally complex and similar contaminated areas.

Funding

This work has been supported by LISBOA-01-0145-FEDER-031863 project, co-funded by FEDER through POR Lisboa (Programa Operacional Regional de Lisboa) from PORTUGAL 2020 and Fundação para a Ciência e a Tecnologia (PTDC/CTA-AMB/31863/2017). The authors gratefully acknowledge the support of CERENA (strategic project FCT-UIDB/04028/2020) and MARE (strategic project FCT-UIDB/04292/2020).

CRediT authorship contribution statement

Renata A. Ferreira: Conceptualization, Investigation (field work and laboratory), Writing (Original Draft and Editing) and Visualization. Manuel F. Pereira: Conceptualization, Methodology, Investigation (field work and mineral geochemical analysis and interpretation), Writing (Original Draft, Review and Editing) and Visualization. João P. Magalhães: Investigation (field work and laboratory) and Visualization. António M. Maurício: Investigation (field work and mineral geochemical analysis and interpretation) and Writing (Review and Editing). Isabel Caçador: Investigation (field work, vegetation survey and species identification) and Writing (Review). Susete Martins-Dias: Conceptualization, Supervision, Writing (Review and Editing) and Funding acquisition.

Declaration of competing interest

The authors declare that they have no known competing financial interests or personal relationships that could have appeared to influence the work reported in this paper.

Acknowledgments

The authors gratefully acknowledge EDM - Empresa de Desenvolvimento Mineiro, S.A., for all the support throughout the work and to Edgar Carvalho for the explanations and follow-up on the field. Also, thanks to João Matos from LNEG for all the personal advises and bibliographic support.

Appendix A. Supplementary material

Supplementary data to this article can be found online at <https://doi.org/10.1016/j.scitotenv.2020.142825>.

References

- Abreu, M.M., Tavares, M.T., Batista, M.J., 2008. Potential use of *Erica andevalensis* and *Erica australis* in phytoremediation of sulphide mine environments: São Domingos, Portugal. *J. Geochem. Explor.* 96,210-222. <https://doi.org/10.1016/j.gexplo.2007.04.007>.
- Abreu, M.M., Santos, E.S., Magalhães, M.C., Batista, M.J., 2012. São Domingos mine wastes phytostabilization using spontaneous plant species. In: Batista, M.J. (Ed.), *Field Guidebook: Multidisciplinary Contribution for Environmental Characterization and Improvement at the S. Domingos Mining Site*. 9th ISEG - International Symposium of Environmental Geochemistry, Aveiro, pp. 42-49. <http://hdl.handle.net/10400.9/1777>.
- Aciego Pietri, J.C., Brookes, P.C., 2008. Relationships between soil pH and microbial properties in a UK arable soil. *Soil Biol. Biochem.* 40, 1856-1861. <https://doi.org/10.1016/j.soilbio.2008.03.020>.
- Alef, K., Nannipieri, P., 1995. S - estimation of microbial activities. In: Alef, K., Nannipieri, P. (Eds.), *Methods in Applied Soil Microbiology and Biochemistry*. Academic Press, London, pp. 193-270.
- Alkorta, I., Aizpurua, A., Riga, P., Albizu, I., Amézaga, I., Garbisu, C., 2003. Soil enzyme activities as biological indicators of soil health. *Rev. Environ. Health* 18, 65. <https://doi.org/10.1515/REVEH.2003.18.1.65>.
- Álvarez-Valero, A.M., Pérez-López, R., Matos, J., Capitán, M.A., Nieto, J.M., Sáez, R., et al., 2008. Potential environmental impact at São Domingos mining district (Iberian Pyrite Belt, SW Iberian Peninsula): evidence from a chemical and mineralogical characterization. *Environ. Geol.* 55, 1797-1809. <https://doi.org/10.1007/s00254-007-1131-x>.
- Anawar, H.M., Freitas, M.C., Canha, N., Santa Regina, I., 2011. Arsenic, antimony, and other trace element contamination in a mine tailings affected area and uptake by tolerant plant species. *Environ. Geochem. Health* 33, 353-362. <https://doi.org/10.1007/s10653-011-9378-2>.
- András, P., Matos, J.X., Turisová, I., Batista, M.J., Kanianska, R., Kharbish, S., 2018. The interaction of heavy metals and metalloids in the soil-plant system in the São Domingos mining area (Iberian Pyrite Belt, Portugal). *Environ. Sci. Pollut. Res.* 25, 20615-20630. <https://doi.org/10.1007/s11356-018-2205-x>.
- Arenas-Lago, D., Santos, E.S., Carvalho, L.C., Abreu, M.M., Andrade, M.L., 2018. *Cistus monspeliensis* L. as a potential species for rehabilitation of soils with multielemental contamination under Mediterranean conditions. *Environ. Sci. Pollut. Res.* 25, 6443-6455. <https://doi.org/10.1007/s11356-017-0957-3>.
- ASTM, 2001. C136-01, Standard Test Method for Sieve Analysis of Fine and Coarse Aggregates. American Society for Testing and Materials. American Society for Testing and Materials, West Conshohocken, PA.
- ASTM, 2014. D1140-14, Standard Test Methods for Determining the Amount of Material Finer than 75-µm (No. 200) Sieve in Soils by Washing. American Society for Testing and Materials. American Society for Testing and Materials, West Conshohocken, PA.
- Bååth, E., 1989. Effects of heavy metals in soil on microbial processes and populations (a review). *Water Air Soil Pollut.* 47, 335-379. <https://doi.org/10.1007/BF00279331>.
- Bini, C., 2011. *Environmental Impact of Abandoned Mine Waste: A Review*. Nova Science Publishers Inc, New York, p. 92.
- Blaud, A., Menon, M., van der Zaan, B., Lair, G.J., Banwart, S.A., 2017. Chapter five - effects of dry and wet sieving of soil on identification and interpretation of microbial community composition. In: Banwart, S.A., DLBT-AiA, Sparks (Eds.), *Quantifying and Managing Soil Functions in Earth's Critical Zone*. 142. Academic Press, pp. 119-142.
- Bojórquez-Quintal, E., Escalante-Magana, C., Echevarría-Machado, I., Martínez-Estévez, M., 2017. Aluminum, a friend or foe of higher plants in acid soils. *Front. Plant Sci.* 8, 1767. <https://doi.org/10.3389/fpls.2017.01767>.
- Buira, A., Carapeto, A., García Murillo, P.G., Monteiro-Henriques, T., 2019. *Adenocarpus lainzii*. The IUCN Red List of Threatened Species. , p. 2019. <https://doi.org/10.2305/IUCN.UK.2019-3.RLTS.T102819637A102819646.en>.
- Camíña, F., Trasar-Cepeda, C., Gil-Sotres, F., Leirós, C., 1998. Measurement of dehydrogenase activity in acid soils rich in organic matter. *Soil Biol. Biochem.* 30, 1005-1011. [https://doi.org/10.1016/S0038-0717\(98\)00010-8](https://doi.org/10.1016/S0038-0717(98)00010-8).
- Carter, M.R., Gregorich, E.G., 2007. *Soil Sampling and Methods of Analysis*. CRC Press, Boca Raton, p. 1264.
- Chou, I.M., Seal, R.R., Wang, A., 2013. The stability of sulfate and hydrated sulfate minerals near ambient conditions and their significance in environmental and planetary sciences. *J. Asian Earth Sci.* 62, 734-758. <https://doi.org/10.1016/j.jseas.2012.11.027>.
- Cogran, P., 2018. Jarosite. Reference Module in Earth Systems and Environmental Sciences. Elsevier <https://doi.org/10.1016/B978-0-12-409548-9.10960-1>.
- Desborough, G.A., Smith, K.S., Lowers, H.A., Swayze, G.A., Hammarstrom, J.M., Diehl, S.F., et al., 2010. Mineralogical and chemical characteristics of some natural jarosites. *Geochim. Cosmochim. Acta* 74, 1041-1056. <https://doi.org/10.1016/j.gca.2009.11.006>.
- Dick, W.A., Cheng, L., Wang, P., 2000. Soil acid and alkaline phosphatase activity as pH adjustment indicators. *Soil Biol. Biochem.* 32, 1915-1919. [https://doi.org/10.1016/S0038-0717\(00\)00166-8](https://doi.org/10.1016/S0038-0717(00)00166-8).
- Dinis, M.D.L., Fiúza, A., Futuro, A., Leite, A., Martins, D., Figueiredo, J., et al., 2020. Characterization of a mine legacy site: an approach for environmental management and metals recovery. *Environ. Sci. Pollut. Res.* 27, 10103-10114. <https://doi.org/10.1007/s11356-019-06987-x>.
- Dold, B., 2014. Evolution of acid mine drainage formation in Sulphidic mine tailings. *Minerals* 4, 621-641. <https://doi.org/10.3390/min4030621>.
- EDM, 2019. Empresa de Desenvolvimento Mineiro, SA. Environmental Remediation of the São Domingos Mine. <https://edm.pt/en/noticias/environmental-rehabilitation-of-sao-domingos-mine-advances-to-the-2nd-stage/> (Accessed 16 of November 2019).
- Eivazi, F., Tabatabai, M.A., 1988. Glucosidases and galactosidases in soils. *Soil Biol. Biochem.* 20, 601-606. [https://doi.org/10.1016/0038-0717\(88\)90141-1](https://doi.org/10.1016/0038-0717(88)90141-1).
- EPA, 1990. Engineering Bulletin: Soil Washing Treatment. United States Environmental Protection Agency, p. 10 EPA/54/2-90/017. <https://frtr.gov/matrix-2019/documents/Soil-Washing/1990-Soil-Washing-Treatment.pdf> (Accessed 11 September 2020).
- Fall, A.C.A.L., 2019. Pyrite, jarosite and iron oxide formation and crystallinity in Acid Sulfate Soils of Senegal, West Africa. 21st EGU General Assembly. Geophysical Research Abstracts. 21, p. 91.
- Figueiredo, M.O., da Silva, T.P., 2011. The positive environmental contribution of jarosite by retaining lead in acid mine drainage areas. *Int. J. Environ. Res. Public Health* 8, 1575-1582. <https://doi.org/10.3390/ijerph8051575>.

- Government-of-Ontario, 2011. Soil, Ground Water and Sediment Standards for Use Under Part XV.1 of the Environmental Protection Act. <https://www.ontario.ca/page/soil-ground-water-and-sediment-standards-use-under-part-xv1-environmental-protection-act> (Accessed 18 December 2019).
- GPMS, 2020. Guide of the Portuguese Geological and Mines Sites. <http://www.roiteirode Minas.pt/local.aspx?v=f295530b-c37f-4866-ac7e-8ab11677dad> (Accessed 10 May 2020).
- Grattan, S.R., Griever, C.M., 1998. Identification and description of soils containing very coarse fractions. *J. Hortic.* 78, 127-157. [https://doi.org/10.1016/S0304-4238\(98\)00192-7](https://doi.org/10.1016/S0304-4238(98)00192-7).
- Günal, E., Erdem, H., Demirbaş, A., 2018. Effects of three biochar types on activity of β -glucosidase enzyme in two agricultural soils of different textures. *Arch. Agron. Soil Sci.* 64, 1963-1974. <https://doi.org/10.1080/03650340.2018.1471205>.
- Gupta, R.K., Abrol, I.P., Finkl, C.W., Kirkham, M.B., Arbestain, M.C., Macías, F., et al., 2008. *Soil mineralogy*. In: Chesworth, W. (Ed.), *Encyclopedia of Soil Science*. Springer Netherlands, Dordrecht, pp. 678-686.
- Huang, L., Baumgartl, T., Mulligan, D., 2012. Is rhizosphere remediation sufficient for sustainable revegetation of mine tailings? *Ann. Bot.* 110, 223-238. <https://doi.org/10.1093/aob/mcs115>.
- IPMA, 2020. Climate Normals 1981-2010. Beja. Instituto Português do Mar e da Atmosfera <https://www.ipma.pt/en/oclima/normais.clima/1981-2010/002>. (Accessed 27 April 2020).
- Kaczyńska, G., Borowik, A., Wyszowska, J., 2015. Soil dehydrogenases as an indicator of contamination of the environment with petroleum products. *Water Air Soil Pollut.* 226, 372. <https://doi.org/10.1007/s11270-015-2642-9>.
- Kerolli-Mustafa, M., Mandić, V., Ćurković, L., Šipušić, J., 2016. Investigation of thermal decomposition of jarosite tailing waste. *J. Therm. Anal. Calorim.* 123, 421-430. <https://doi.org/10.1007/s10973-015-4881-9>.
- Kulhawy, F.H., Chen, J.-R., 2009. Identification and description of soils containing very coarse fractions. *J. Geotech. Geoenviron.* 135, 635-646. [https://doi.org/10.1061/\(ASCE\)1090-0241\(2009\)135:5\(635\)](https://doi.org/10.1061/(ASCE)1090-0241(2009)135:5(635)).
- LOIP, 2020. LOSS-ON-IGNITION PROTOCOL. <http://pasternack.ucdavis.edu/research/methods/loss-ignition-protocol> (Accessed 14 May 2019).
- Long, D.T., Fegan, N.E., Mckee, J.D., Lyons, W.B., Hines, M.E., Macumber, P.G., 1992. Formation of alunite, jarosite and hydrous Iron-oxides in a hypersaline system - Lake Tyrrell, Victoria, Australia. *Chem. Geol.* 96, 183-202. [https://doi.org/10.1016/0009-2541\(92\)90128-R](https://doi.org/10.1016/0009-2541(92)90128-R).
- Margesin, R., Schinner, F., 1994. Phosphomonoesterase, phosphodiesterase, phosphotriesterase, and inorganic pyrophosphatase activities in forest soils in an alpine area: effect of pH on enzyme activity and extractability. *Biol. Fertil. Soils* 18, 320-326. <https://doi.org/10.1007/BF00570635>.
- Matos, J.X., Soares, S., Claudino, C., 2006. Caracterização Geológica-geotécnica da corta da mina de São Domingos, FPL X Congresso Nacional Geotecnia, SPG/UNL. 3. Universidade Nova de Lisboa, pp. 741-752.
- Matos, J.X., Pereira, Z., Batista, M.J., De Oliveira, D., 2012. São Domingos mining site - Iberian Pyrite Belt. In: Batista, M.J. (Ed.), *Field Guidebook: Multidisciplinary Contribution for Environmental Characterization and Improvement at the S. Domingos Mining site*. 9th ISEG - International Symposium of Environmental Geochemistry, Aveiro, pp. 7-12. <http://hdl.handle.net/10400.9/1773>.
- Murray, J., Kirschbaum, A., Dold, B., Guimarães, E.M., Miner, E.P., 2014. Jarosite versus soluble Iron-sulfate formation and their role in acid mine drainage formation at the Pan de Azúcar mine tailings (Zn-Pb-Ag), NW Argentina. *Minerals* 4, 477-502. <https://doi.org/10.3390/min4020477>.
- Oades, J.M., 1993. The role of biology in the formation, stabilization and degradation of soil structure. *Geoderma* 56, 377-400. [https://doi.org/10.1016/0016-7061\(93\)90123-3](https://doi.org/10.1016/0016-7061(93)90123-3).
- Oggerin, M., Rodríguez, N., Moral, C.d., Amils, R., 2014. Fungal jarosite biomineralization in Rio Tinto. *Res. Microbiol.* 165, 719-725. <https://doi.org/10.1016/j.resmic.2014.10.001>.
- Orczewska, A., Piotrowska, A., Lemanowicz, J., 2012. Soil acid phosphomonoesterase activity and phosphorus forms in ancient and post-agricultural black alder [*Alnus glutinosa* (L.) Gaertn.] woodlands. *Acta Soc. Bot. Pol.* 81, 81-86. <https://doi.org/10.5586/asbp.2012.013>.
- Pansu, M., Gautheryrou, J., 2006. *Handbook of Soil Analysis; Mineralogical, Organic and Inorganic Methods*. Springer-Verlag Berlin Heidelberg <https://doi.org/10.1007/978-3-540-31211-6>.
- Paz-Ferreiro, J., Trasar-Cepeda, C., Leirós, M.C., Seoane, S., Gil-Sotres, F., 2009. Biochemical properties in managed grassland soils in a temperate humid zone: modifications of soil quality as a consequence of intensive grassland use. *Biol. Fertil. Soils* 45, 711-722. <https://doi.org/10.1007/s00374-009-0382-y>.
- Paz-Ferreiro, J., Trasar-Cepeda, C., del Carmen Leirós, M., Seoane, S., Gil-Sotres, F., 2011. Intra-annual variation in biochemical properties and the biochemical equilibrium of different grassland soils under contrasting management and climate. *Biol. Fertil. Soils* 47, 633-645. <https://doi.org/10.1007/s00374-011-0570-4>.
- Pereira, R., Antunes, S.C., Marques, S.M., Gonçalves, F., 2008. Contribution for tier 1 of the ecological risk assessment of Cunha Baixa uranium mine (Central Portugal): I. Soil chemical characterization. *Sci. Total Environ.* 390, 377-386. <https://doi.org/10.1016/j.scitotenv.2007.08.051>.
- Pérez-López, R., Álvarez-Valero, A.M., Nieto, J.M., Sáez, R., Matos, J.X., 2008. Use of sequential extraction procedure for assessing the environmental impact at regional scale of the São Domingos Mine (Iberian Pyrite Belt). *Appl. Geochem.* 23, 3452-3463. <https://doi.org/10.1016/j.apgeochem.2008.08.005>.
- Quental, L., Brito, M.G., Sousa, A.J., Abreu, M.M., Batista, M.J., Oliveira, V., et al., 2003. Utilização de imagens hiperespectrais na avaliação da contaminação mineira em S. Domingos, Faixa Piritosa, Alentejo. VI Congresso Nacional de Geologia, Monte de Caparica, Universidade Nova de Lisboa, Faculdade de Ciências e Tecnologia, pp. M33-M36. <http://hdl.handle.net/10400.9/1030>.
- Rejsek, K., Vranova, V., Pavelka, M., Formanek, P., 2012. Acid phosphomonoesterase (EC 3.1.3.2) location in soil. *J. Plant Nutr. Soil Sci.* 175, 196-211. <https://doi.org/10.1002/jpln.201000139>.
- Rosado, L., Morais, C., Candeias, A.E., Pinto, A.P., Guimarães, F., Mirão, J., 2008. Weathering of S. Domingos (Iberian Pyrite Belt) abandoned mine slags. *Mineral. Mag.* 72, 489-494. <https://doi.org/10.1180/minmag.2008.072.1.489>.
- Sánchez España, J., López Pamo, E., Santofimia, E., Aduvire, O., Reyes, J., Baretino, D., 2005. Acid mine drainage in the Iberian Pyrite Belt (Odiel river watershed, Huelva, SW Spain): geochemistry, mineralogy and environmental implications. *Appl. Geochem.* 20, 1320-1356. <https://doi.org/10.1016/j.apgeochem.2005.01.011>.
- Santos, E.S., Abreu, M.M., Magalhães, M.C.F., 2016. *Cistus ladanifer* phytostabilizing soils contaminated with non-essential chemical elements. *Ecol. Eng.* 94, 107-116. <https://doi.org/10.1016/j.ecoleng.2016.05.072>.
- Scarlett, N.V.Y., Grey, I.E., Brand, H.E.A., 2012. *Fundamental studies into the formation of jarosite related precipitates*. EP126758. *Engineering, CSIRO Process Science and Engineering*.
- Smith, J.L., Doran, J.W., 1996. Measurement and use of pH and electrical conductivity for soil quality analysis. In: Doran, J.W., Jones, A.J. (Eds.), *Methods for Assessing Soil Quality*. Soil Science Society of America Madison, pp. 169-185. <https://doi.org/10.2136/sssaspecpub49.c10>.
- Stotzky, G., Broder, M.W., Doyle, J.D., Jones, R.A., 1993. Selected methods for the detection and assessment of ecological effects resulting from the release of genetically engineered microorganisms to the terrestrial environment. In: Neidleman, S., Laskin, A.I. (Eds.), *Advances in Applied Microbiology*. 38. Academic Press, pp. 1-98. [https://doi.org/10.1016/S0065-2164\(08\)70214-4](https://doi.org/10.1016/S0065-2164(08)70214-4).
- Tabatabai, M.A., Bremner, J.M., 1969. Use of p-nitrophenyl phosphate for assay of soil phosphatase activity. *Soil Biol. Biochem.* 1, 301-307. [https://doi.org/10.1016/0038-0717\(69\)90012-1](https://doi.org/10.1016/0038-0717(69)90012-1).
- Tabatabai, M.A., Bremner, J.M., 1970. Arylsulfatase activity of soils I. *Soil Sci. Soc. Am. J.* 34, 225-229. <https://doi.org/10.2136/sssaj1970.03615995003400020016x>.
- Turner, B.L., 2010. Variation in pH optima of hydrolytic enzyme activities in tropical rain Forest soils. *Appl. Environ. Microbiol.* 76, 6485-6493. <https://doi.org/10.1128/aem.00560-10>.
- Turner, B.L., Hopkins, D.W., Haygarth, P.M., Ostle, N., 2002. β -Glucosidase activity in pasture soils. *Appl. Soil Ecol.* 20, 157-162. [https://doi.org/10.1016/S0929-1393\(02\)00020-3](https://doi.org/10.1016/S0929-1393(02)00020-3).
- visitmertola, 2015. Mina de S. Domingos; Mining Heritage. <https://visitmertola.pt/en/item/mina-de-s-domingos-the-mining-route/> (Accessed 10 May 2020).
- von Mersi, W., Schinner, F., 1991. An improved and accurate method for determining the dehydrogenase activity of soils with idonitrotetrazolium chloride. *Biol. Fertil. Soils* 11, 216-220. <https://doi.org/10.1007/BF00335770>.
- Whalen, J., Warman, P., 1996. Arylsulfatase activity in soil and soil extracts using natural and artificial substrates. *Biol. Fertil. Soils* 22, 373-378. <https://doi.org/10.1007/BF00334586>.
- WS, 2020. Wet Sieving: A Practical Guide. <https://www.globalgilson.com/blog/wet-sieving-practical-guide> (Accessed 12 May 2020).

This is a post-peer-review version of an article published in *Science of The Total Environment*, 2021 following peer review. The version of record Ferreira, R., Pereira, M., Magalhães, J., Maurício, A., Caçador, I. & Martins-Dias, S. (2021). Assessing local acid mine drainage impacts on natural regeneration-revegetation of São Domingos mine (Portugal) using a mineralogical, biochemical and textural approach. *Science of The Total Environment*, 755, 1-16. <https://doi.org/10.1016/j.scitotenv.2020.142825>